

**Annual Report
(Year 1: 1999-2000)**

**Advanced Algorithms and Automation Tools for Discrete Ordinates
Methods in Parallel Environments
(DOE NEER Grant DE-FG07-991D13779)**

by

A. Haghighat (haghighat@psu.edu)

Nuclear Engineering Program
Mechanical and Nuclear Engineering Department
The Pennsylvania State University
231 Sackett Building
University Park, PA 16802
(814) 865-0039
(814) 865-8499

(June 22, 2000)

Table of Contents

I. Executive Summary

II. Work Done in 1999-2000

II.1 Studies on adaptive differencing strategy

II.2 Angular Multigrid Acceleration For Parallel S_n Method

II.3 Expert system for automation of model preparation in a parallel environment

III. Proposed work for 2000-2001

- Itemizes tasks
- Personnel

References

I. Executive summary

This project develops methodologies, algorithms, and automation tools for solving the 3-D linear Boltzmann (“transport”) equation¹ based on the discrete ordinates technique in parallel environments.

The discrete ordinates (Sn) method² is one of the most accurate and versatile techniques used to solve the “integro-differential” form of the Boltzmann equation. The method, however, requires a significant amount of computer time and memory. To overcome this difficulty, new parallel computing architectures have to be exploited. Effective parallel Sn algorithms, acceleration formulations and iterative techniques are needed. Further, to save in engineer’s time in developing “effective” models, especially for a real-life problem, an “expert” system is needed that accounts for both numerical and parallel processing factors. In summary, with this project, we are developing methods and tools that significantly reduce both computer and engineer’s time.

In the first year of the project, we have performed the following three tasks:

- 1) Demonstrated the effectiveness and necessity of an adaptive differencing strategy based on the three Kobayashi 3-D benchmark problems.(Refs. 3-5) Findings of this study is used for our efforts in tasks 2 and 3.
- 2) Developed different angular multigrid acceleration algorithms; incorporated these algorithms into the PENTRAN code, and examined the effectiveness of these algorithms for different problem physics using the Kobayashi benchmark problem 1. Thus far, combinations of Simplified Angular Multigrid (SAM), Nested Iteration (NI), and V-Cycle angular multigrid algorithms have proved to be very effective for a large range of c-ratios. We have achieved speedups as high as a factor of ~7.3 in the number of iterations, or a factor of ~4.0 in the CPU time. Preliminary studies indicate that other combinations such as SAM+V-cycle+PCR or NI+V-cycle+PCR can be even more effective in certain problem conditions. (Refs. 6 and 7)
- 3) Initiated development of an algorithm for an “expert” system for generation of mesh distribution for 3-D Sn transport codes operating in a parallel environment. Thus far, we have developed a semi-analytical formulation based on the first collision source that provides the general solution behavior throughout the problem. This is necessary in order to be able to choose an appropriate mesh and differencing scheme. A computer program called PENFC (Parallel Environment Neutral-particle First Collision) has been developed. We have examined different numerical options for solving the semi-analytical formulation, and measured the accuracy and performance of the different numerical techniques compared to the Kobayashi benchmark problem 1.

II. Work done in 1999-2000

II.1 Studies on adaptive differencing strategy:

To investigate the effectiveness of adaptive differencing strategy, we have used the three Kobayashi 3-D benchmark problems that were developed for examining the accuracy of 3-D transport codes. These problems are parallelepiped or cubic in shape and contain three regions: source, void, and shield. Problems are solved for two situations: i) the material in the source and shield regions is a pure absorber; ii) the materials in the source and shield regions have a 50% scattering ratio. The total cross-section of this material is 0.1 cm^{-1} , while the total cross-section of the void is 10^{-4} cm^{-1} . These problems, despite of their simplicity in material and geometry, are very

challenging for the Sn method because of two main reasons: 1) Particle flux drops by several orders of magnitude; 2) A purely or low scattering material generally result in the “ray-effects”.

We have solved all the problems with the PENTRAN code (Ref. 8). PENTRAN includes an adaptive differencing strategy which allows for the use of different differencing schemes including LD (linear diamond) linear fit, DTW (directional theta-weighted) linear fit, and the EDW (exponential directional weighted) exponential fit, depending on problem physics and/or user’s choice. We achieve close agreement with the reference analytical solutions, and have demonstrated that the use of the adaptive differencing strategy is necessary in order to obtain solutions with minimal “ray-effects”. (Refs. 4 and 5) This is accomplished by considering following measures: i) Refined meshes are used within and in the vicinity of the source; ii) Coarse meshes are considered away from the source, so that larger spatial cells intercept angular rays as they spread out, thereby reducing the “ray-effects”; iii) Adaptive differencing strategy is used: DTW is used in the source and void regions, and EDW is used in the coarse meshes within the pure absorber and low scattering shield regions.

For example, Fig. 1 shows problem 3, referred to as the shield with dog-leg void duct, composed of three regions: source, void ducts, and shield. The problem size is $60 \times 100 \times 60 \text{ cm}^3$, the cubic source region is $10 \times 10 \times 10 \text{ cm}^3$, and void duct penetrates through model.

Fig. 2 compares the PENTRAN Sn results to the analytical solutions along x-axis at every 10 cm between 5 and 55 cm, at $y = 95 \text{ cm}$ and $z = 35 \text{ cm}$. The maximum difference of $<26\%$ occurs at $x = 15 \text{ cm}$ in a flux value that is smaller than by more than four orders of magnitude relative to the source. Note that the Sn solutions are calculated in $\sim 20 \text{ sec}$ on one processor of the Penn State PC-Cluster (i686 processor) using a S20 level-symmetric quadrature set.

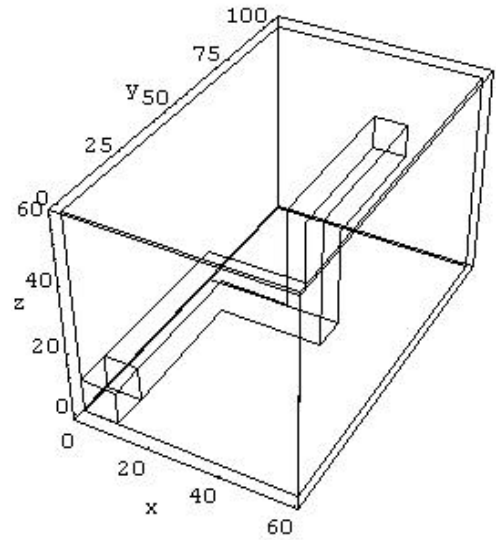


Fig. 1 – Schematic of Kobayashi benchmark problem 3

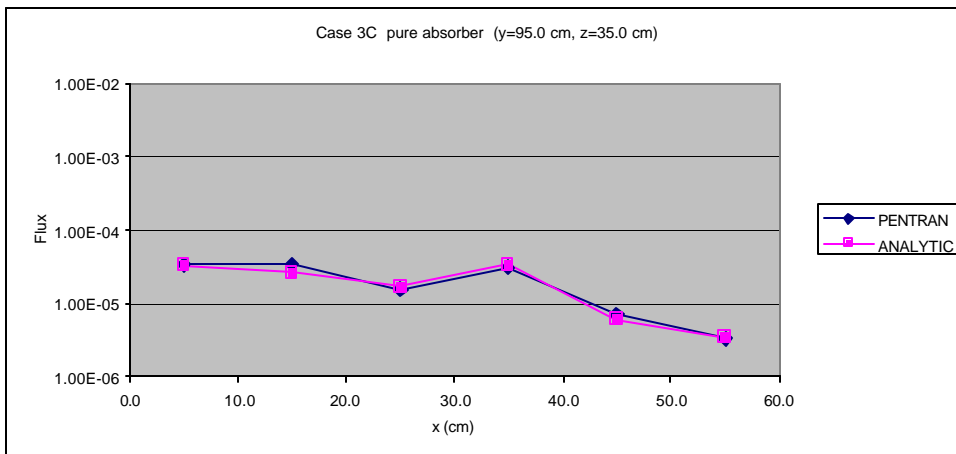


Fig. 2 – A sample comparison of Sn results with analytical solutions

II.2 Angular Multigrid Acceleration For Parallel S_n Method

We have developed (Refs. 6 and 7) different multigrid formulations including the Simplified Angular Multigrid (SAM), Nested Iteration (NI), and V-Cycle algorithms, and their various combinations with and without the standard acceleration scheme of partial current rebalance (PCR). These algorithms solve the S_n formulation for different angular grid orders q (Ω^q)

$$\frac{|m_m|^q}{\Delta x}(\Psi_{out,x}^q - \Psi_{in,x}^q) + \frac{|h_m|^q}{\Delta y}(\Psi_{out,y}^q - \Psi_{in,y}^q) + \frac{|x_m|^q}{\Delta z}(\Psi_{out,z}^q - \Psi_{in,z}^q) + \mathbf{s}\Psi_A^q = S_A^q, \quad (1)$$

where S_A^q includes scattering, external and fission sources. For all algorithms, when it is needed to project coarse-grid (Ω^q) angular fluxes onto the fine-grid (Ω^{q+1}), i.e., $\tilde{\Psi}^{q+1} = P^{q \rightarrow q+1} \Psi^q$, we select the angular flux in a particular direction on Ω^q that is closest to a direction on Ω^{q+1} . This is accomplished by finding the minimum angle between direction vectors of Ω^q and Ω^{q+1} :

$$\cos(\mathbf{a}_{m,n}^{q \rightarrow q+1}) = \mathbf{m}_m^q \mathbf{m}_n^{q+1} + \mathbf{h}_m^q \mathbf{h}_n^{q+1} + \mathbf{x}_m^q \mathbf{x}_n^{q+1} \quad \text{where} \quad \begin{aligned} n &= 1, \dots, N(N+2) \in \Omega^{q+1} \\ m &= 1, \dots, M(M+2) \in \Omega^q, M < N \end{aligned} \quad (2)$$

In case there is more than one minimum angle, the angular fluxes are determined by performing simple arithmetic mean of the fluxes in these directions. To calculate the errors in the coarse-grid angular fluxes, the fine-grid residuals in the source moments are used.

Finally, in order to conserve particles, we normalize the projected angular fluxes by using the

$$\text{following balance equation: } \Psi_n^{q+1} = \tilde{\Psi}_n^{q+1} \frac{\sum_{m=1}^{M(M+2)} w_m^q \Psi_m^q}{\sum_{n=1}^{N(N+2)} w_n^{q+1} \tilde{\Psi}_n^{q+1}}.$$

Below, we will discuss the formulations and performance of the different angular multigrid algorithms developed in this study.

a. Simplified Angular Multigrid (SAM)

This is a */cycle* multigrid formulation, which is called the Simplified Angular Multigrid (SAM) scheme. In the SAM scheme, a global approximate solution (i.e., angular fluxes) is obtained on a coarse angular grid (e.g., S₄/ P₀, P₁), and then this solution is projected (source moments and boundary angular fluxes) onto a fine angular grid (e.g., S₁₀/ P₅) filtering out the low frequency error components. Effectively, the calculation on the coarse-grid provides preconditioning for the fine-grid iterations

b. Nested Iteration (NI)

A variation of the SAM scheme is the *Nested Iteration*, in which we use successively refined multiple angular grids (e.g., Ω^{8h} , Ω^{6h} , Ω^{4h} , Ω^{2h} , Ω^h). We start on the coarsest angular grid (e.g., Ω^{8h}) and solve for angular fluxes within certain convergence tolerance. These angular fluxes are then used as the initial solution for the next finer grid. This process is continued until we converge on the finest grid (Ω^h).

c. V-Cycle

In the V-cycle algorithm, we, first perform an iteration on the fine angular grid, and compute the difference between the previous and the current iteration scattering sources for each cell and

direction. This difference is called the *residual*. Residuals are then expanded into moments to be used as source on the next coarse angular grid. We then perform a sweep on the coarse angular grid to render the error terms. This process is continued until we reach the prescribed coarsest grid. Using the *closest direction* approach, these error terms are projected back to the fine-grid to update the angular fluxes and the scattering source. We then proceed to the next iteration with the updated source. We cycle among the selected grids until a converged solution on the fine angular grid is obtained. The angular multigrid V-Cycle formulation is described below:

- Sweep $H^{q+1}\Psi^{q+1} = S^{q+1}$ on Ω^q with the initial guess Ψ^{q+1}
- Compute residual $r^{q+1} = q^{q+1} - q_{old}^{q+1}$
- Sweep $H^q e^q = P^{q+1 \rightarrow q} r^{q+1}$ on Ω^{q+1} with the initial guess $e^{q+1} = 0$
- Update fluxes $\tilde{\Psi}^{q+1} = \Psi^{q+1} + P^{q \rightarrow q+1} e^q$ and scattering source $q^{q+1} \rightarrow \tilde{q}^{q+1}$
- Sweep $H^{q+1}\Psi^{q+1} = \tilde{q}^{q+1}$ on Ω^{q+1} with the initial guess $\tilde{\Psi}^{q+1}$

where H is the transport operator, r is the residual, e is the error, P is the projection operator, and *tilde* represents the updated values.

d. Combinations of V-Cycle with the SAM and NI formulations

We have used SAM and NI formulations to obtain starting guess for the V-Cycle formulation. Figure 2 depicts the V-Cycle, and its combinations with SAM and NI.

PERFORMANCE OF MULTIGRID FORMULATIONS

We have implemented the new multigrid algorithms into our

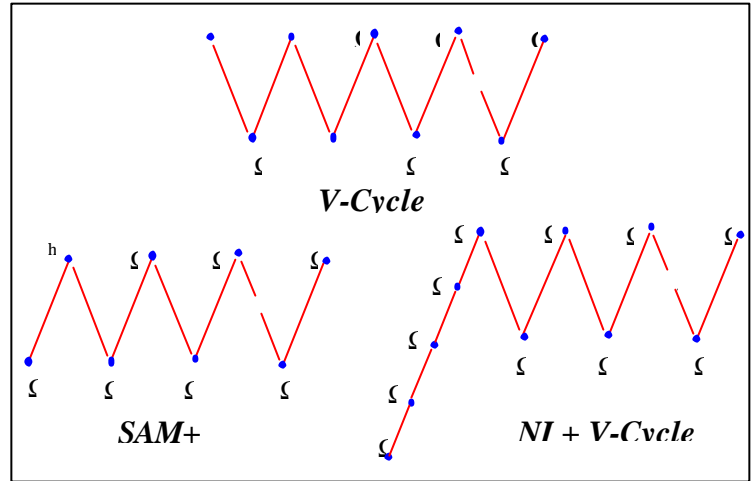


Figure 2: V-cycle and its combination with SAM and NI

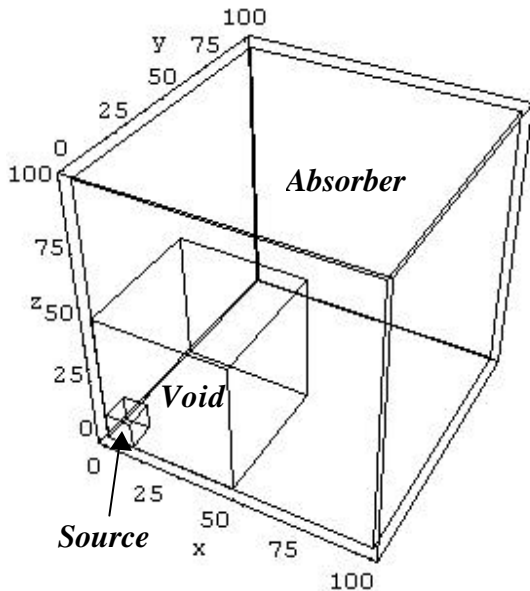


Figure 3: Kobayashi benchmark problem 1

PENTRANTM (Parallel Environment Neutral-particle TRANsport) 3-D parallel Sn code, and measured performance using the Kobayashi benchmark problem 1 (Ref. 3), Fig. 3. We have investigated the effect of a variety of physical parameters, including different scattering ratios, coarse- and fine-grid convergence tolerances and angular quadrature orders.

Using the findings of Section II.1, we have developed PENTRAN models for this problem. We have analyzed cases with different c-ratios ranging from 0.6 to 0.99 using a level-symmetric

quadrature set. To examine the effect of parallel processing, we have partitioned the angular domain into four subdomains (2 octants/ processor) and processed them on 4 processors of the LIONX parallel PC Cluster at Penn State University.

The results of these studies have been presented in detail in Refs. 6 and 7. Here, we provide a brief discussion on our important findings.

Effect of Coarse- and Fine-grid Tolerances

For the SAM algorithm, for the c-ratio in a range of 0.6-1.0 and fine-grid tolerances of $1.e-04 - 1.e-6$, the coarse-grid tolerance should be in a range of $1.e-03 - 1.e-04$.

Effect of c-ratio

SAM becomes more effective with the increasing c-ratio, resulting in a significant acceleration as high as ~ 7.8 . SAM outperforms PCR by a factor of ~ 2.6 in iteration speed-up, however it requires significant (~ 2.6) computation time than the PCR.

Effect of Coarse- and Fine-grid Quadrature Orders

This study indicates that for an effective acceleration for problems with fine-grid quadrature orders up to S_{10} , the coarse-grid quadrature order should be either S_6 or S_8 , considering the degree of the problem's angular dependency. Beyond S_{10} for the fine-grid, the coarse-grid quadrature orders should not be greater than S_8 or S_{10} .

Combinations of Angular Multigrid Formulations

In Table 1, we summarize various combinations of the angular multigrid formulations and the

Table 1: Comparison of speedups obtained by combined formulations^a

Algorithm	ITERATION SPEED-UP	CPU SPEED-UP
NO ACCELERATION	1.00	1.00
PCR	2.43	2.38
SAM	2.76	1.52
SAM+PCR	5.41	3.24
NESTED	1.83	1.37
NESTED+PCR	5.62	3.39
V	1.74	1.28
V+PCR	4.87	3.43
V+SAM	3.24	1.57
V+SAM+PCR	7.30	3.39
V+NESTED	2.76	1.58
V+NESTED+PCR	6.95	2.45

^a $c\text{-ratio}=0.6$, S_{10} for coarse-grid, S_{20} for fine-grid, S_4 to S_{10} for the NI coarse-grids, and coarse- and fine-grid convergence tolerances of $5.e-02$ and $5.e-04$, respectively.

PCR acceleration. These tests have been performed for a c-ratio of 0.6, coarse and fine-grid tolerances and quadrature orders of $5.e-02/5.e-04$, and S_{10}/S_{20} , respectively. For the Nested Iteration (NI), we have started on S_4 , gradually upgrading to S_{10} . Table 1 indicates that angular multigrid formulations combined with PCR become very effective. SAM combined with PCR reduces the CPU by a factor of ~ 3.43 , while PCR alone reduces by a factor of ~ 2.38 . The combination of V-

cycle, SAM and PCR can significantly reduce number of fine-grid iterations, however, because of the high cost of V-cycle, is not as effective in reducing the CPU time.

II.3 Expert system for automation of model preparation in a parallel environment

In this section, we discuss our efforts in developing an expert system that automatically develops an effective model considering both numerical and parallel processing factors. This task significantly impacts engineer's time, reliability of results, and eventually computing time.

Following flow-chart depicts the major component of this expert system.

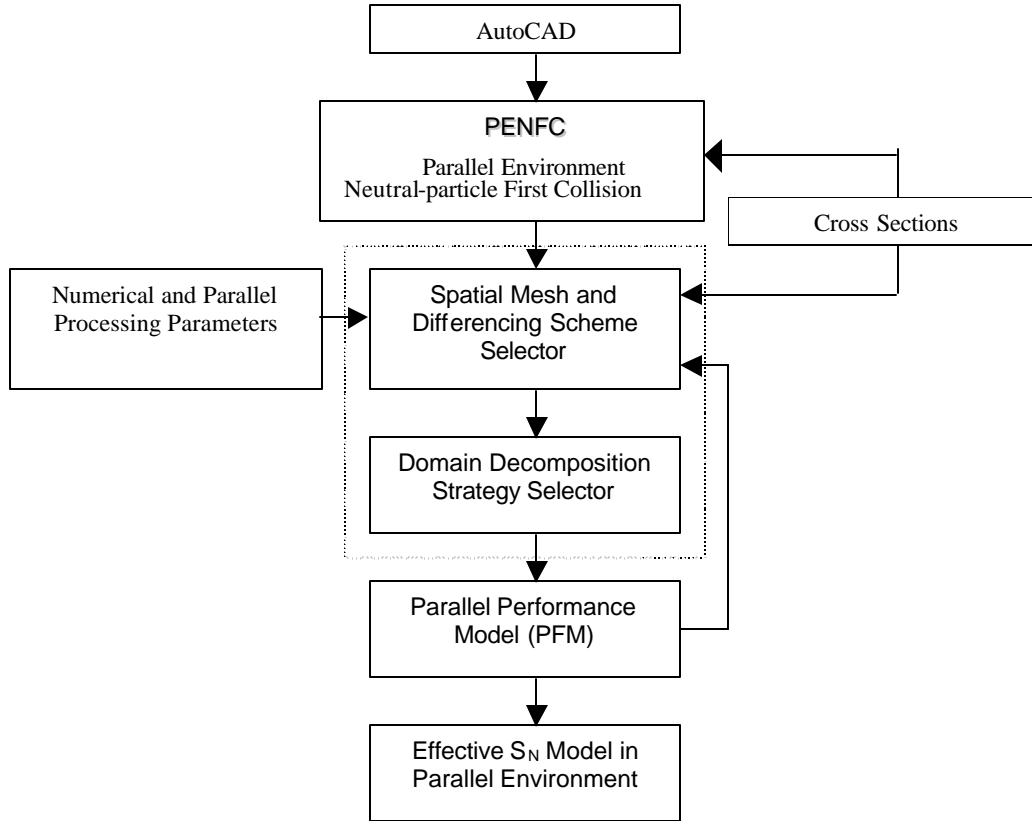


Fig. 4 – Flow-chart of the expert system for automation of model preparation in parallel environments

To date, we have developed a program to determine an initial flux distribution based on the first collided neutrons. To reduce the computational time of this program, we have developed a parallel version using the MPI (message passing interface) library. Below, we provide a brief discussion the PENFC (Parallel Environment Neutral-particle First Collision) algorithm and its testing.

Formulation of uncollided flux in a 3-D geometry

Uncollided fluxes at any position \underline{r} inside a 3-D model can be calculated by

$$\mathbf{f}_g^u(\underline{r}) = \frac{1}{4\pi} \int_{V_s} d\underline{r}' \frac{S_g(\underline{r}') e^{-\int_0^{|\underline{r}-\underline{r}'|} \Sigma_{t,g}(\underline{r}'') d\underline{r}''}}{|\underline{r}' - \underline{r}|^2} \quad (3)$$

where g is the energy group index, $\phi_g^u(\underline{r})$ is the uncollided flux of the energy group g , $S_g(\underline{r}')$ is the source strength (n/cm³/s) of the energy group g , $\sigma_{t,g}$ is the total cross section of the energy group g , V_s is the volume of the source region, and $d\underline{r}'$ is the volume element.

We have solved Eq. 3 via two approaches: spatial discretization and numerical integration.

a. Spatial Discretization

We discretize the volume of the whole model into a number of fine meshes, and rewrite Eq. (3) as

$$\mathbf{f}_g^u(\underline{r}) = \frac{1}{4p} \sum_{i=1}^P \frac{S_{g,i} e^{-\int_0^{|\underline{r}-\underline{r}_i|} \mathbf{s}_{t,g}(\underline{r}') d\underline{r}'}}{|\underline{r}_i - \underline{r}|^2} \quad (4)$$

where P is the total number of source points, and $S_{g,i} = V_i S_g$ is the intensity (n/s) of a point source of the energy group g at the center of a fine mesh, and S_g is the average source strength (n/cm³/s) of the energy group g within V_i volume of the fine mesh.

b. Numerical Integration

Following some mathematical manipulation, Eq. 3 in spherical system of coordinate reduces to

$$\mathbf{f}_g^u(\underline{r}) = \frac{S_g}{4p \mathbf{s}_{t,g,0}} \int_0^{2p} d\mathbf{j} \int_0^p d\mathbf{q} \sin \mathbf{q} \left[e^{-\mathbf{s}_{t,g,1} l_a} (1 - e^{-\mathbf{s}_{t,g,0} (l_b - l_a)}) \right] \quad (5)$$

where S_g is the source strength (n/cm³/s) of the energy group g that is constant throughout the source volume, l_a is the path length from the position \underline{r} to the boundary of the source region and $l_b - l_a$ is the path length inside the source region, $\mathbf{s}_{t,g,0}$ is the total cross section of the source region of the energy group g and $\mathbf{s}_{t,g,1}$ is the total cross section of the region outside the source region of the energy group g .

To solve the above double integrals, thus far, we have investigated three quadrature formulations including trapezoidal, Simpson, and 3/8-formula, and concluded that the trapezoidal method is the most effective approach.

Benchmarking of PENFC

We have examined the performance and accuracy of the PENFC based on the Kobayashi 3-D benchmark problem 1, as was used in Section II.2. Table 2 presents a sample comparison of the PENFC results with the reference analytical solutions along the main diagonal of the model for the two solution approaches.

Table 2

Flux distribution along the main diagonal of the Kobayashi benchmark problem 1

Position (cm)	Analytical solution	Spatial Discretization (1.0-cm mesh)		Numerical Integration (Trapezoidal)	
		Uncollided	% Difference	Uncollided	% Difference
5,5,5	5.957E+00	5.952E+00	-0.073	5.956E+00	-0.006
15,15,15	4.708E-01	4.661E-01	-0.993	4.698E-01	-0.213
25,25,25	1.700E-01	1.691E-01	-0.540	1.697E-01	-0.158
35,35,35	8.683E-02	8.645E-02	-0.447	8.670E-02	-0.154
45,45,45	5.251E-02	5.230E-02	-0.406	5.243E-02	-0.155
55,55,55	1.334E-02	1.329E-02	-0.343	1.332E-02	-0.133
65,65,65	1.459E-03	1.455E-03	-0.245	1.457E-03	-0.114
75,75,75	1.754E-04	1.750E-04	-0.208	1.752E-04	-0.099
85,85,85	2.246E-05	2.242E-05	-0.181	2.244E-05	-0.097
95,95,95	3.010E-06	3.005E-06	-0.163	3.008E-06	-0.087

Both methods yield accurate solutions, while within and in the vicinity of the source, the discretized method requires significantly more detailed meshing, and therefore considerably more computation time. Based on these analyses, we have concluded that the numerical integration approach is a more effective methodology for our application. Currently we are examining the use of PENFC for solving real-life problems.

III. Proposed Work: YEAR 2: 2000-20001

For the year 2 of this project, we propose to perform the following tasks:

Task 1. Acceleration scheme

- Further testing of the multigrid formulations for real-life problems, such as the VENUS-3 benchmark problem (Ref. 9) and a BWR core shroud simulation (Ref. 10), and analytical analyses of these algorithms for ideal problems. (Students 1 and 2)
- Initiate development of a parallel Simplified Pn (SPn) algorithm. (Student 2)

Task 2. Iterative techniques

- Examination of other ADS algorithms considering different domain decomposition strategies for different nuclear properties and boundary conditions. (Student 1)
- Development of different multi-coloring iterative techniques, and measuring their performance for different physical problems. (Student 2)

Task 3. Expert system for automation of input preparation

- Further testing of the PENFC performance for real-life problems such as the VENUS-3 benchmark problem; if needed, we will test the Gaussian quadrature formulation. (Student 3)
- Develop an algorithm for combining PENFC flux derivatives with the adaptive differencing strategy for selection of appropriate differencing schemes. (Student 3)
- Initiate development of a “performance modeling” algorithm considering different domain decomposition strategies. (Student 3)

Personnel

Prof. Alireza Haghighat and three graduate students from the Penn State Nuclear Engineering Program will perform the above tasks. They will be assisted by Dr. Glenn E. Sjoden (US Air Force) who is the primary author of PENTRAN.

Note that one of the students will be funded under another grant, and for Dr. Sjoden, we are only asking for funds for two one-week trips.

REFERENCES

1. W. Greenberg and P. Polewczak, "Modern Mathematical Methods in Transport Theory," Operator Theory: Advances and Applications Vol. 51, *Birkhauser Verlag*, 1991.
2. E.E. Lewis and W.F. Miller, Computational Methods of Neutron Transport, *John Wiley & Sons, Inc.*, 1984.
3. K. Kobayashi, "A Proposal for 3-D Radiation Transport Benchmark for Simple Geometries with Void Region," *OECD Proceedings of 3-D Deterministic Radiation Transport Computer Programs*, 403-413, Paris, France (1996)
4. A. Haghighat and G.E. Sjoden, "Kobayashi Benchmarks using PENTRAN™," *Proc. Mathematics and Computation*, Madrid, Spain, (1999).
5. A. Haghighat, G.E. Sjoden, and V. Kucukboyaci, "Effectiveness of PENTRAN's Unique Numerics for Simulation of the Kobayashi Benchmarks," submitted for publication in the special issue of the *Progress in Nuclear Energy*, March, 2000.
6. V. Kucukboyaci and A. Haghighat, "Simplified Angular Multigrid Method to Accelerate S_n Calculations," *Transaction of American Nuclear Society*, Vol. 81, 140-144, Nov. 14-18, 1999, Long Beach, CA.
7. V. Kucukboyaci and A. Haghighat, "Angular Multigrid Acceleration For Parallel S_n Method With Application To Shielding Problems," *Proceedings of the PHYSOR 2000 Conference*, May 7-11, 2000, Pittsburgh, PA.
8. G.E. Sjoden and A. Haghighat, "PENTRAN - A 3-D Cartesian Parallel S_n Code with Angular, Energy, and Spatial Decomposition," *Proceedings of the 1997 Joint International Conference on Mathematical Methods and Supercomputing for Nuclear Applications*, Vol. 1, 553, Saratoga Springs, NY (1997).
9. A. Haghighat, A. Abderrahim, and G.E. Sjoden, "Accuracy and Parallel Performance of PENTRAN Using the VENUS-3 Benchmark Experiment", *Reactor Dosimetry*, ASTM STP 1398, John G. Williams, et al., Eds., ASTM, West Conshohocken, PA, 2000.
10. V. Kucukboyaci, A. Haghighat, G. E. Sjoden and B. Petrovic, "Modeling of BWR for Neutron and Gamma Fields Using PENTRAN," *Reactor Dosimetry*, ASTM STP 1398, John G. Williams, et al., Eds., ASTM, West Conshohocken, PA, 2000.